Modal Structure, Directional and Wavelength Jumps of Integrated Semiconductor Ring Lasers: Experiment and Theory.

S. Fürst,[1] A. Pérez-Serrano,[2] A. Scirè,[2] M. Sorel,[1] and S. Balle[3]

[1]*Dept. of Electronics and Electrical Engineering, University of Glasgow, Glasgow, United Kingdom.*
[2]*Instituto de Física Interdisciplinar y Sistemas Complejos, IFISC (CSIC-UIB), Palma de Mallorca, Spain.*
[3]*Institut Mediterrani d'Estudis Avançats, IMEDEA (CSIC-UIB), Esporles, Spain.*

(Dated: 12th June 2008)

We have experimentally and theoretically analyzed the modal properties of semiconductor ring lasers and the wavelength jumps that occur in connection with directional switching above threshold.

For many years, semiconductor ring lasers (SRLs) have attracted interest for their potential in the fabrication of micro-cavity lasers and densely integrated photonics circuits. It has recently been realized that the coexistence of two counterpropagating modes in the same gain medium leads to a large variety of operating regimes and dynamics that are profoundly different from those of Fabry-Perot lasers [1]. One of the most interesting property is the extremely fast directional bistability that opens up a new scenario in the development of all-optical memories and signal processing [2, 3]. Besides their switching characteristics, SRLs show several unexpected behaviors such as hysteresis in the lasing direction [4, 5] and atypical lasing mode selection rules [6]. In particular, when current or temperature are changed, the lasing mode does not hop between consecutive cavity modes but exhibits sudden jumps between several cavity modes only when the lasing direction reverses. This characteristic strongly enhances the stability of the lasing wavelength against changes in the operating conditions.

In this letter we report on the measurement of the transfer function of SRL devices, which provides us with a map of the cavity resonances, and the emission wavelength of the SRLs when biased above threshold. The transfer function can be theoretically explained by considering the perturbation induced by the light-extraction sections, which induces a symmetry breaking in the resonant cavity and a modulation of the cavity losses. For the geometry considered, the cavity losses have a wavelength periodicity that corresponds to three ring cavity modes, which explains the measured hops in wavelength as the bias current of the laser is increased.

The devices were fabricated using a shallow etched technology on a multiple quantum well AlGaInAs/InP metal-organic chemical vapor deposition (MOCVD) wafer, as described in [7]. The device layout (see Fig. 1) consists of a ring cavity with a ring radius of 300 μm, coupled to a straight output waveguide by a point evanescent coupler. The waveguides are 2 μm wide and the gap between the ring and the output waveguides is 750 nm, providing a theoretical coupling ratio of 12%. To minimize the backreflections, the output waveguides are 10° tilted to the cleaved facets.

For analyzing the cavity resonances of the SRL, we inject through port #1 a monochromatic field from a tunable laser and we measure the photo-current generated in ports #3 and #4, which are reverse biased (see Fig. 1). During these measurements, the ring is biased close to transparency to minimize the losses. The power collected at port #3 as the input wavelength is scanned (positive peaks in Fig. 2) displays narrow and well defined peaks at wavelengths equispaced by 0.4 nm. The peak heights show the expected profile defined by the wavelength-dependent gain spectrum in the structure but also an additional modulation that occurs every three longitudinal modes.

Measurements over different devices show that the longitudinal modes possess a doublet structure, with the splitting between the two subpeaks varying from 1 GHz to 4 GHz. In addition, for a particular device, the split-

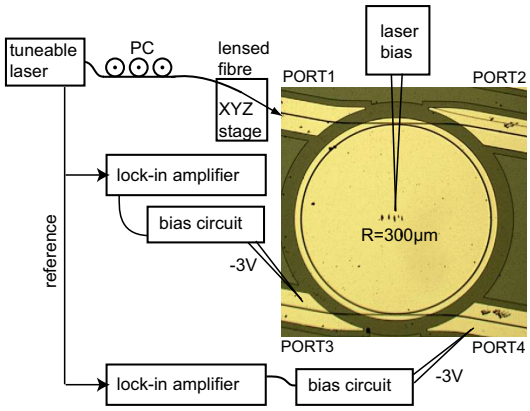

Figure 1: Optical micrograph of a 300 μm-radius ring laser with the corresponding measurement setup.

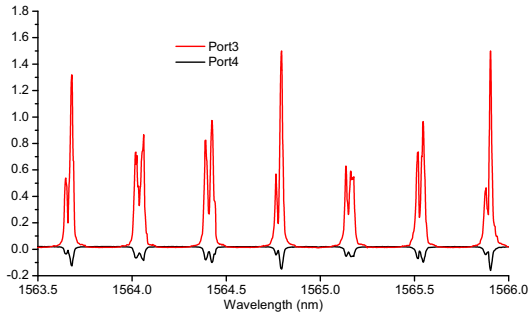

Figure 2: Detected power (arbitrary units) at port #3 and #4.

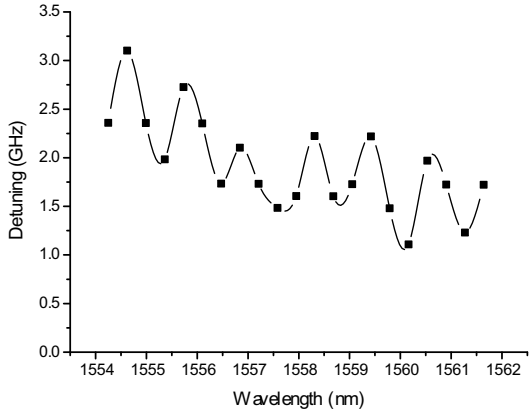

Figure 3: Measured splitting between doublets.

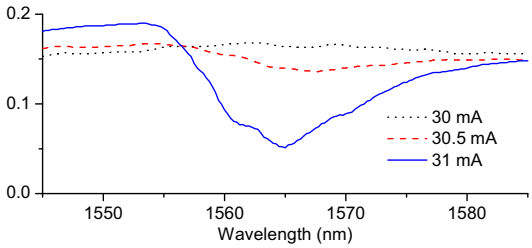

Figure 4: Current dependence of the dips at port #4.

ting between the subpeaks usually displays a modulation that corresponds with the additional modulation in the longitudinal mode spectrum described above. Fig. 3 shows the measured doublet splitting for another device, which displays a modulation that also corresponds to a periodicity of roughly three mode spacings.

The power collected at port #4 (negative peaks in Fig. 2) presents a similar structure with the same periodicity, but instead of displaying peaks, it shows dips on the spontaneous-emission noise background. It is worth remarking that the depth of the dips strongly depends on the bias current in the SRL cavity (see Fig. 4): the dips cannot be seen for bias currents below 30.5 mA, but they are visible above this current.

When the laser is biased above threshold, the main lasing direction does not remain stable for all current values. The L-I curve for the device in Fig. 3 shows periodic switching between CW and CCW emission for increasing current, a generic behavior in this type of devices [4]. Additionally, the dominant lasing wavelength remains constant except for a small thermal drift between switches, but it suddenly jumps by three cavity modes when the lasing direction reverses, as shown in Fig. 5.

These experimental results can be explained by computing the transfer matrix of the complete SRL structure [8]. We assume that the two couplers are identical, lossless and with a residual reflectivity due to their point-like character. Small reflectivity from output facets #1 and #2 is included, but not from #3 or #4 since the corresponding output waveguides are reverse biased. From

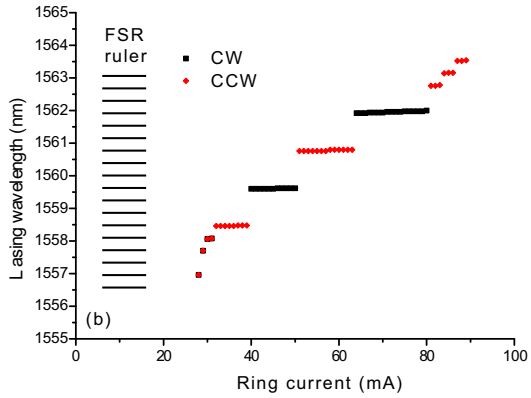

Figure 5: Lasing wavelength as a function of SRL current.

this analysis, the roundtrip condition for the SRL modes in a resonator with equal arms of length $L/2$ can be formulated as

$$\mathrm{e}^{2iqL} - a\mathrm{e}^{iqL} + b = 0 \,, \tag{1}$$

where q is the complex propagation constant. In (1), $b = (r_u r'_u - t_u t'_u)^{-1}(r_d r'_d - t_d t'_d)^{-1}$, $a = (r_u r_d + r'_u r'_d + t'_u t_d + t_u t'_d)b$, $t_{u(l)}$ and $r_{u(l)}$ denote the frequency-dependent transmittivity and reflectivity of the upper (lower) coupler for CW waves, and primed symbols denote the same magnitudes for CCW waves. Defining $Q_\pm = a/2 \pm \left[(a/2)^2 - b\right]^{1/2}$, the SRL modes are given by

$$q_m^\pm L = 2\pi m - i \ln Q_\pm \,. \tag{2}$$

The light-extraction section breaks the circular symmetry of the SRL [9], destroying the pure CW and CCW states at $q_m = 2\pi m$. Two branches of solutions emerge due to the term $-i \ln Q_\pm$, which correspond to the experimentally observed doublets. Their splitting normalized to the free-spectral range of the SRL is thus given by

$$\Delta = \frac{1}{2\pi}\left\{\mathrm{Im}\left[\ln\left(\frac{Q_-}{Q_+}\right)\right] - \alpha \mathrm{Re}\left[\ln\left(\frac{Q_-}{Q_+}\right)\right]\right\} \,, \tag{3}$$

α being the linewidth enhancement factor.

The theoretical results for the power at port #3 are in good agreement with the results shown in Fig. 2 provided that a small amount of gain in the SRL is included (see Fig. 6). In these calculations, the section lengths have been taken from the device layout and facet reflectivities have been adjusted to match the experimental results.

The results for the transfer matrix to port #4 show similar trends, and the transfer matrix analysis does not lead to dips on an spontaneous-emission noise background. The reason is that the transfer matrix analysis does not include spontaneous emission noise in the SRL cavity. Indeed, due to the (slight) gain in the SRL, the power collected at ports #3 and #4 in the absence of external light is the power due to spontaneous emission in the SRL, including amplification and attenuation in

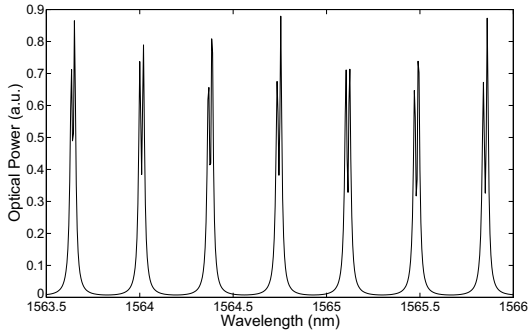

Figure 6: Theoretical calculation of the power collected at port # 3.

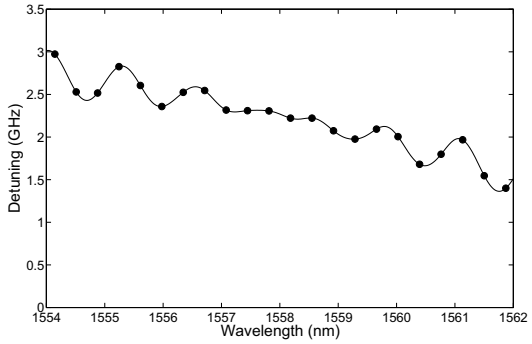

Figure 7: Theoretical detuning between doublets.

the path. In the absence of any reflecting element, light injected into the SRL through port #1 would reach port #3 only after being amplified or attenuated along the path, and no injected light would reach port #4; however, the power at port #4 would be reduced because of amplified spontaneous emission (ASE) suppression under light injection, thus leading to dips onto the ASE background. It is worth remarking that this effect provides us with a precise way to measure the spectral dependence of the transparency current.

In the same way, we can compute the theoretical detuning for the device used in Figs. 3 and 5 (see Fig. 7). The modulation of the detuning at three mode spacings is apparent, arising from the residual reflectivity at the bends of the output waveguides. In addition, it presents a further slow modulation that arises from the finite effective length of the output couplers and their residual reflectivities.

Finally, the modal selection above threshold can be explained from (1) and (3) by considering the modulation imposed by the cavity losses together with the red-shift of the gain due to Joule heating of the laser junction. For $\alpha \gtrsim 2$–3, the maximum frequency splitting of the doublets almost coincides with their maximum threshold difference, whose modulation for each branch is out of phase. Hence, when the gain spectrum redshifts due to Joule heating, the system will jump from the minimum on one branch to the following minimum on the other branch. For circular SRL, where $L \geq 2R$, this means a jump of $m = int[3\tau_R/\tau_{FP}]$ modes of the SRL, where $\tau_{R(FP)}$ is the roundtrip time in the SRL (Fabry-Perot) cavity. Thus, for the device considered here, the modal jumps correspond to $m = 3$.

In summary, we have experimentally studied the modal structure of SRLs by measuring the transfer properties of the device below threshold and the wavelength jumps that occur in connection with directional switching above threshold. A transfer matrix analysis explains the measurements when amplified spontaneous emission in the SRL cavity is accounted for. The residual reflectivities in the light extraction sections determine the frequency splitting and threshold difference between the two branches of solutions. This effect together with the redshift of the material gain explain the wavelength jumps displayed by the SRL above threshold.

We acknowledge financial support from project IOLOS, ref. # 034743, FP6-2005-IST-5, PhoDeCC TEC2006-10009/MIC, QULMI PROGECIB-5A and TEC2006-13887-C05-03.

[1] M. Sorel, G. Giuliani, A. Scirè, R. Miglierina, S. Donati and P. J. R. Laybourn, *IEEE J. Quantum Electron.*, **39**(10), pp. 1187–1195, (2003).

[2] V. R. Almeida, C. A. Barrios, R. R. Panepucco, M. Lipson, M. A. Foster, D. G. Ouzounov and A. L. Gaeta, *Opt. Lett.*, **29**, pp. 2867–2870 (2004).

[3] M. T. Hill, H. J. S. Dorren, T. de Vrie, X. J. M. Leijtens, J. H. den Besten, B. Smalbrugge, Y. S. Oei, H. Binsma, G. D. Khoe and M. K. Smit, *Nature*, **432**, pp. 206–209 (2004).

[4] M. Sorel, P. J. R. Laybourn, G. Giuliani and S. Donati, *Appl. Phys. Lett.*, **80**(17), pp. 3051–3053, (2002).

[5] M. F. Booth and A. Schremer and J. M. Ballantyne, *Appl. Phys. Lett.*, **76**(9), pp. 1095–1098, (2000).

[6] C. J. Born, M. Hill, S. Yu and M. Sorel, *Quantum Electronics and Laser Science Conference — QELS 2005*, **2**, pp. 1035, (22–27 May 2005).

[7] S. Fürst and M. Sorel, *IEEE Phot. Tech. Lett.*, **20**(5), pp. 366–368, 2008.

[8] A. E. Siegman, *Lasers*, University Science Books, Mill Valley, CA, pp. 398–426, (1986).

[9] E. J. D'Angelo, E. Izaguirre, G. B. Mindlin, G. Huyet, L. Gil, J. R. Tredicce, *Phys. Rev. Lett.*, **68**(25), pp. 3702-3705, (1992).